**Supplemental Figure 1**

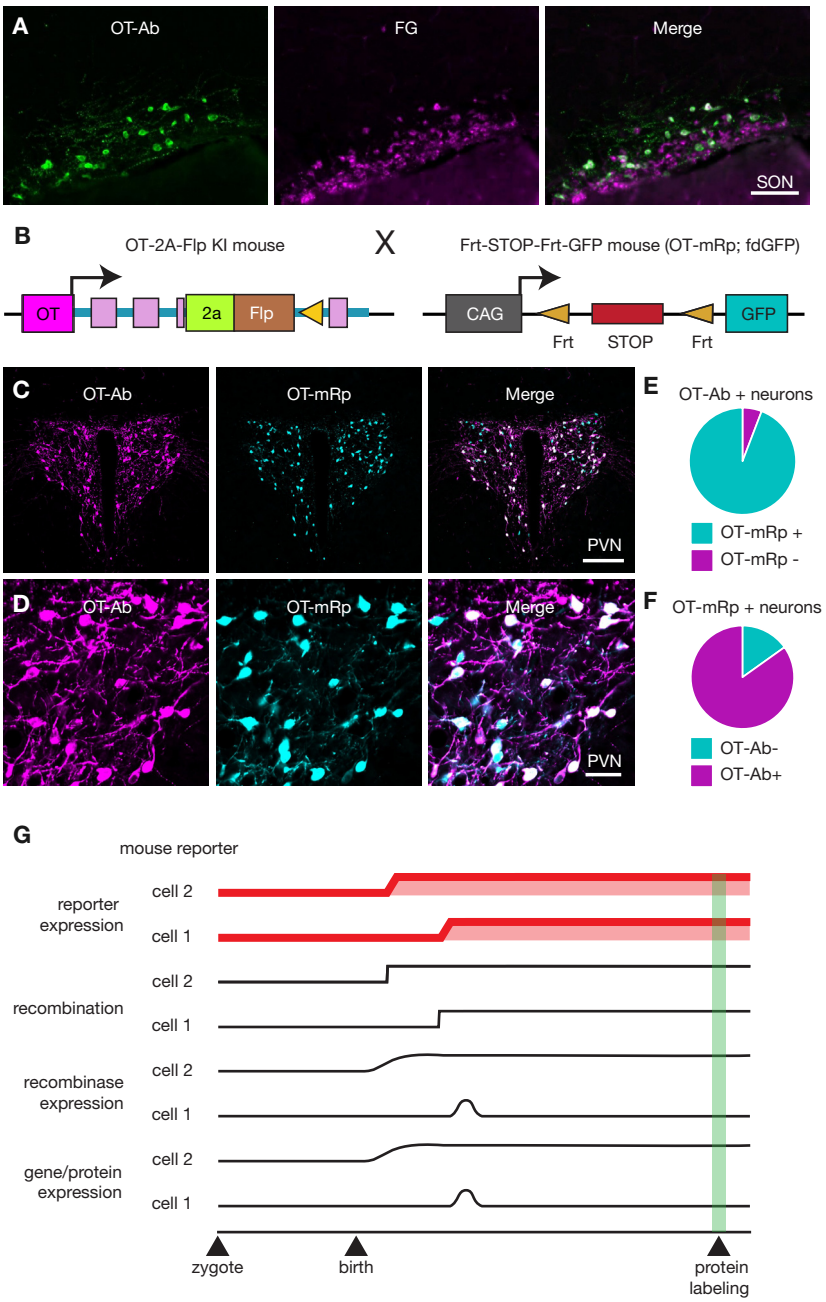


**Supplemental Figure 1. Intravenous FluoroGold labeling in the supraoptic nucleus and validation of OT-2A-Flp::fdGFP cross to label OTergic neurons.** Related to **Figures 1, 2, 3, 6**. (A) Example images of the OT neurons in the supraoptic nucleus (SON) of a i.v. FluoroGold-injected mouse (scale bar 100 μm) showing OT-Ab (green, left), FG (magenta, center) and merged (right) images. (B) Breeding strategy for OT-2A-Flp driver mice crossed to fdGFP reporter mice. (C) OT antibody (OT-Ab, magenta left), GFP (OT-mRP, cyan, center), and merged (right) image of the PVN at low magnification (scale bar 200 μm). (D) OT-Ab (magenta left), OT-mRP (cyan, center), and merged (right) image of the PVN at high magnification (scale bar 50 μm). (E,F) Quantification of the efficacy of the mouse reporter strategy (n = 1 male mouse, P36, 862 neurons counted). OT-Ab positive neurons are 94.2% mRp positive (E). OT-mRp positive neurons are 84.9% OT-Ab positive (F). (G) Once recombination occurs, the reporter gene remains recombined thereafter, and consequently the reporter is expressed even in the absence of ongoing recombinase expression. If the gene that serves as the driver is expressed in some cells (e.g. cell 1), only under appropriate physiological conditions, there will be a partial mismatch between reporter and protein expression.

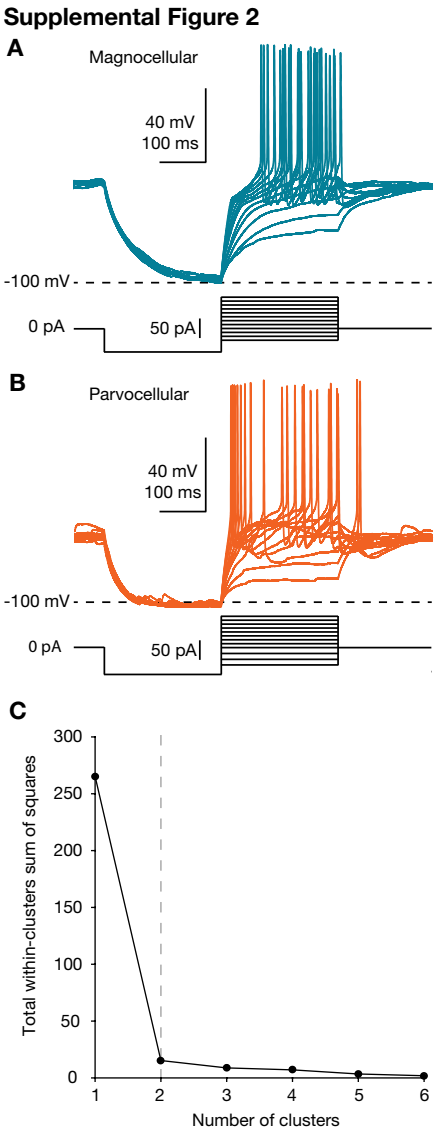


**Supplemental Figure 2. Electrophysiological protocol to distinguish magnocellular and parvocellular OT neurons.** Related to **Figures 2, 6**. (A) Overlay of 12 electrophysiological traces in which a magnocellular OT neuron was hyperpolarized to -100 mV and depolarized from that membrane potential with current steps of increasing amplitude. (B) Overlay of 12 electrophysiological traces in which a parvocellular OT neuron was hyperpolarized to -100 mV and depolarized from that membrane potential using current steps of increasing amplitude. (C) The number of clusters used in the k-means clustering analysis was determined by the elbow method. By this common heuristic, the number of clusters is chosen such that adding more clusters reduces the distance between points and their centroids only marginally. The chosen number of clusters is indicated by the gray dashed line.

**Supplemental Figure 3**

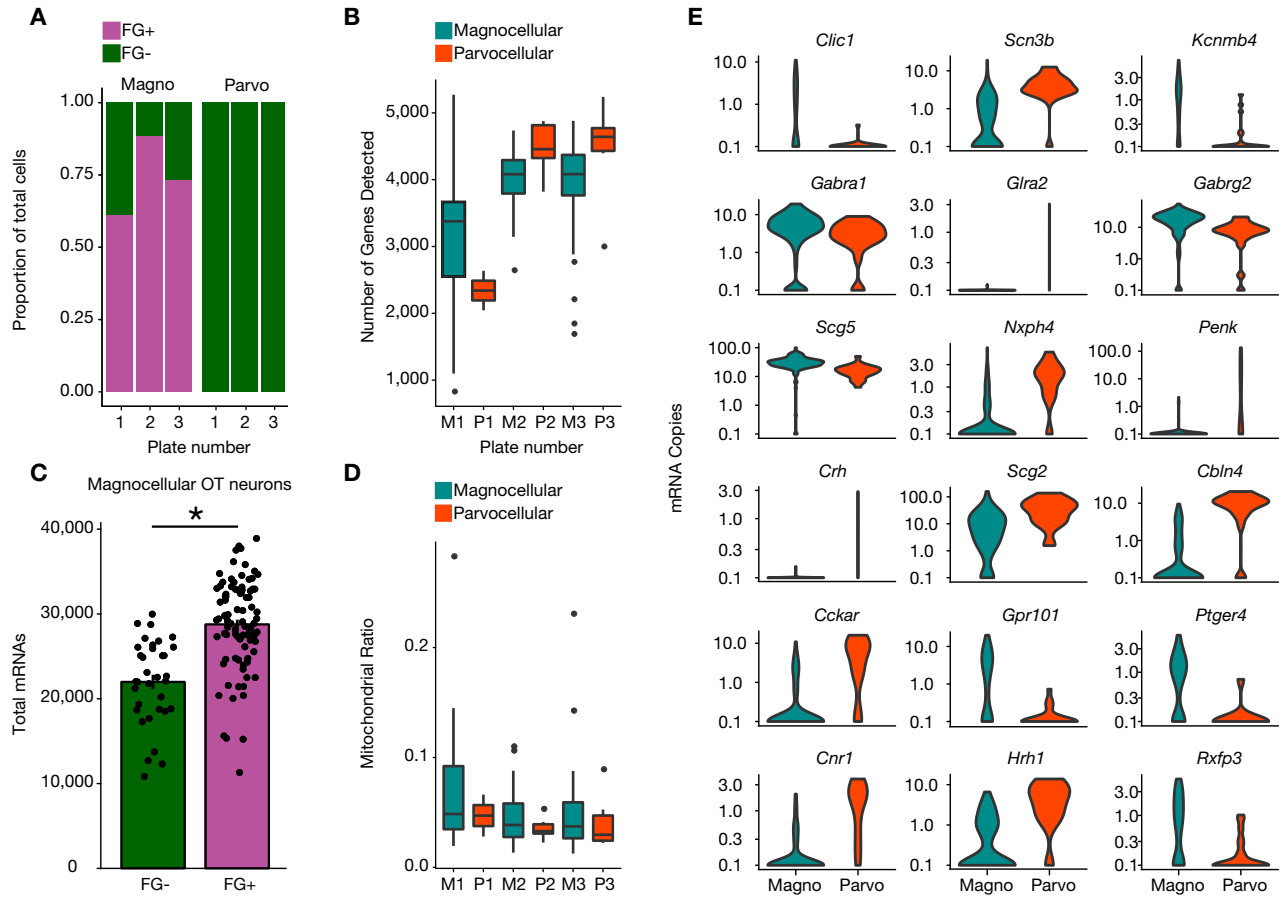


**Supplemental Figure 3. Relation of FluoroGold labeling and mitochondria ratio to scRNAseq clustering and differentially expressed genes that may contribute to electrophysiological properties of magnocellular and parvocellular OT neurons.** Related to **Figure 3, 4**. A) Proportion of each cell type on each plate accounting for FG signal. (B) Number of genes detected in each cell type by plate. (C) Magnocellular OT neurons without detectable i.v. FG labeling contain fewer total mRNAs than magnocellular OT neurons with detectable i.v. FG labeling ($t_{(123)}$ = 6.4904 p = $1.891^{e-09}$). * indicates $p < 0.05$; Pearson's product moment test for statistical comparison (D) The per cell ratio of reads mapped to mitochondrial RNA vs total number of mapped reads by cell type and plate. (E) Hand-curated gene set with potential to influence electrophysiological properties based on the International Union of Basic and Clinical Pharmacology (IUPHAR) (https://www.guidetopharmacology.org/). Categories were intersected with the list of genes significantly (FDR < 0.1%) differentially expressed between the two cell types.

**Supplemental Figure 4**

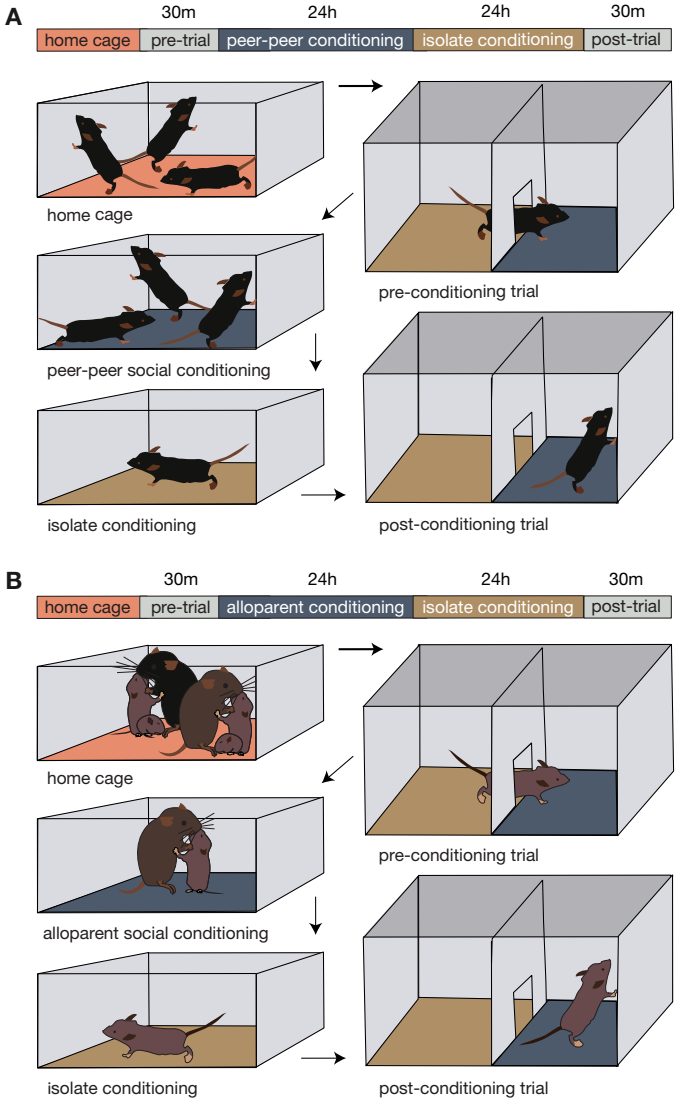


**Supplemental Figure 4. Illustrations of protocols and timelines for social CPP and alloparent CPP assays.** Related to **Figure 5, 7**. (A) social CPP assay. At approximately 6 weeks of age, animals were removed from social housing in a standard cage and placed individually into one of 5 open field activity chambers partitioned into two equally sized zones. Mouse activity and position was monitored by infrared beam breaks. The amount of time each mouse spent exploring each zone was recorded during a 30 min pre-conditioning trial to establish baseline preference for the bedding cues. Immediately after this trial, mice received social conditioning with cage mates for 24 hr on one type of bedding used in the pre-conditioning trial, followed by 24 hr isolation conditioning in on the other bedding. Immediately following the isolation conditioning, a 30 min post-conditioning trial was conducted to establish preference for the two conditioned bedding cues. (B) The alloparent CPP assay was conducted in the same activity chambers using an identical configuration to the social CPP assay. Alloparent stimulus animals were adult virgin wild type C57BL6/J females that were housed with pregnant WT or *Fmr1* KO females prior to the birth of pups. This housing configuration was maintained until alloparent CPP testing began. Beginning at postnatal day 19-20, and continuing until each male littermate was tested, male mice were individually weaned from their home cage and placed directly in an activity chamber with two novel beddings. To establish each animal's baseline preference for the novel bedding cues, the amount spent exploring each zone of the activity chamber was recorded during a 30 min pre-conditioning trial. Immediately after this trial, mice individually received alloparent conditioning with their virgin female alloparent for 24 hr on one type of bedding, followed by 24 hr isolation conditioning on the other type of bedding. Immediately after isolation conditioning, a 30 min post-conditioning trial was conducted to establish preference for the two conditioned bedding cues.

**Supplemental Figure 5**

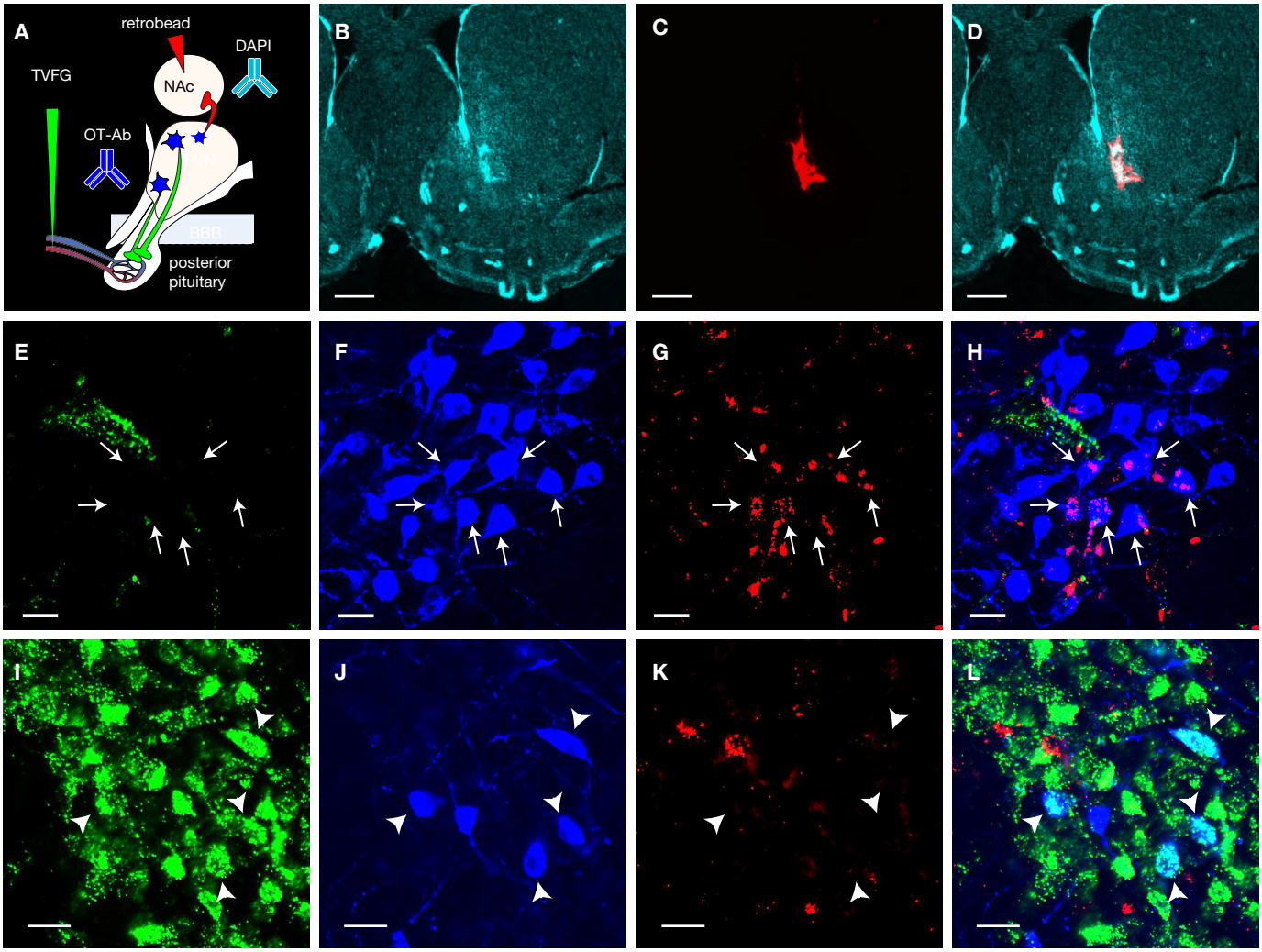


**Supplemental Figure 5. Parvocellular, but not magnocellular OT neurons innervate NAc.** Related to **Figure 6**. (A) Diagram illustrating injection and labeling strategy (B-D) Images of NAc labeled with DAPI (B), RtB (C), and merged (D) showing successful RtB targeting. Scale bar 1 mm. (E-H) Images of caudal PVN labeled with FG (E), OT-Ab (F), RtB (G), and merged (H) showing presence of RtB in FG- OT neurons. Arrows indicate FG-/RtB+ OT neurons. Scale bar 20 μm. (I-L) Images of rostral PVN labeled with FG (I), OT-Ab (J), RtB (K), and merged (L) showing absence of RtBs from FG+ OT neurons. Arrowheads indicate FG+/RtB- neurons. Scale bar 20 μm.

**Supplemental Figure 6**

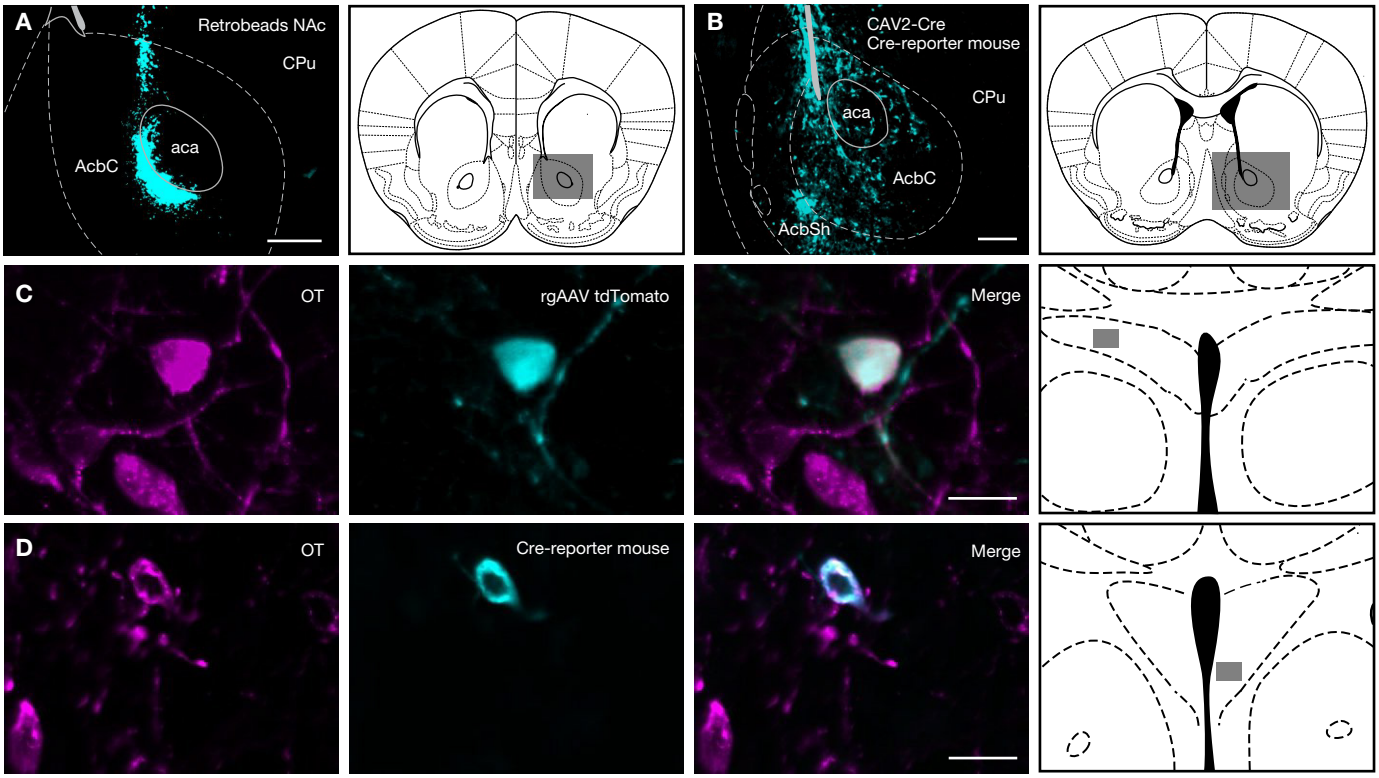


**Supplemental Figure 6. Injection targeting and viral expression.** Related to **Figures 6, 7**. (A) Retrobead injection targeted to NAc (left) and atlas image depicting the area captured in the image (right). (B) CAV2-Cre infection induces Cre-mediated recombination. (left) CAV2-Cre injection targeted to NAc of a tdTomato Cre-reporter mouse and (right) atlas image depicting the area captured in the image. (C) retro-AAV infects PVN OT neurons that innervate NAc. From left to right: OT-Ab; retro-AAV-tdTomato expression; Merge; atlas image indicating the location captured in images to the left. (D) retro-AAV-fdCre can induce Flp-dependent Cre-mediated recombination in PVN OT neurons. From left to right: OT-Ab; Cre-mediated tdTomato expression; Merge; atlas image indicating the location captured in images to the left. Atlas images adapted from Paxinos and Franklin, 2001. Scale bars indicate 200 μm in low magnification images, and 20 μm in high magnification images.

**Supplemental Figure 7**

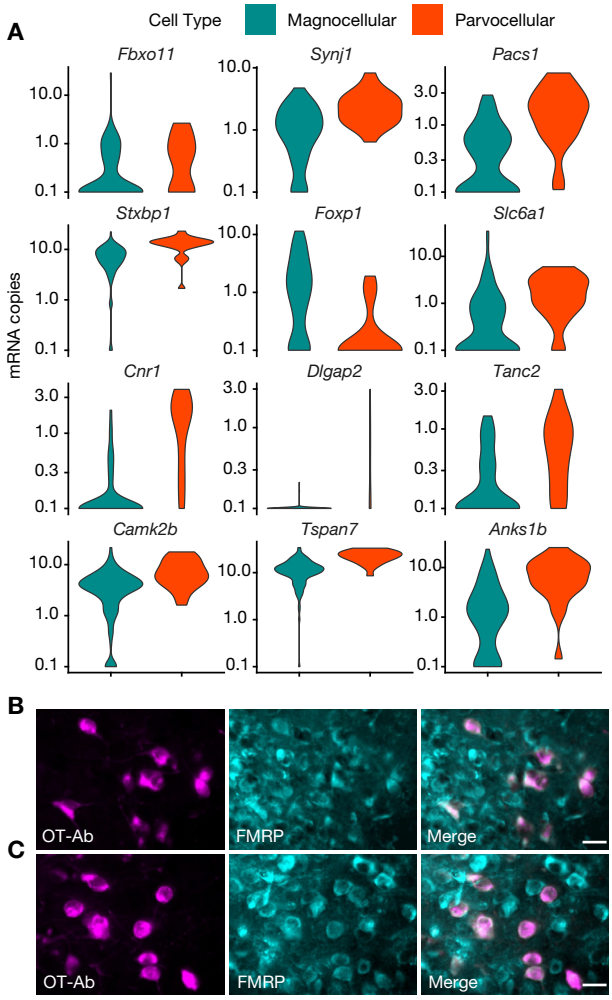


**Supplemental Figure 7. Differentially expressed ASD risk genes that are binding targets of FMRP.** Related to **Figure 8**. (A) Violin plots for the set of 12 differentially expressed ($p < 0.05$) FMRP binding targets that are also ASD risk genes. Of the 12 genes, 10 are enriched in parvocellular OT neurons. (B,C) FMRP is expressed in OT neurons in the rostral (B) and caudal (C) PVN. Scale bar 20 μm. Monocle Likelihood Ratio Test for statistical comparisons.

**Supplemental Figure 8**

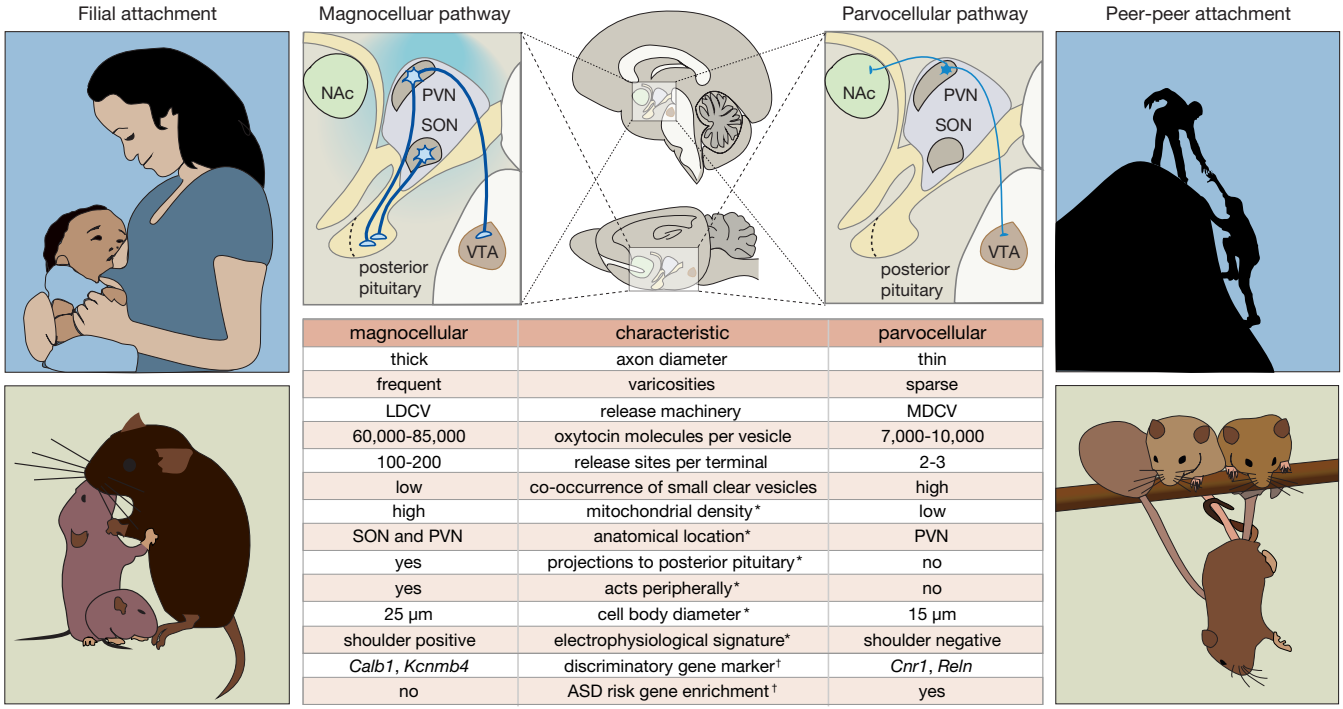


| magnocellular | characteristic | parvocellular |
|---|---|---|
| thick | axon diameter | thin |
| frequent | varicosities | sparse |
| LDCV | release machinery | MDCV |
| 60,000-85,000 | oxytocin molecules per vesicle | 7,000-10,000 |
| 100-200 | release sites per terminal | 2-3 |
| low | co-occurrence of small clear vesicles | high |
| high | mitochondrial density* | low |
| SON and PVN | anatomical location* | PVN |
| yes | projections to posterior pituitary* | no |
| yes | acts peripherally* | no |
| 25 µm | cell body diameter* | 15 µm |
| shoulder positive | electrophysiological signature* | shoulder negative |
| *Calb1*, *Kcnmb4* | discriminatory gene marker† | *Cnr1*, *Reln* |
| no | ASD risk gene enrichment† | yes |

**Supplemental Figure 8. Parallel processing of social behaviors by oxytocin, working model.** Related to **Figure 1, 2, 3, 4, 5, 6, 7, 8**. Cartoon illustration of (Left) filial attachments; (Right) peer-peer attachments; (Center-Top) magnocellular and parvocellular oxytocin release mechanisms, from the hypothalamus to target brain regions, in human (top) and rodent (bottom). (Center-Bottom) Summary table of cellular characteristics used to differentiate between magnocellular and parvocellular oxytocin neurons. Table citations: axon diameter (Zhang and Hernández, 2013); varicosities (Zhang and Hernández, 2013); release machinery (van den Pol, 2012; Zhang et al., 2011, 2009); oxytocin molecules per vesicle (Dreifuss, 1975; Nordmann and Morris, 1984; van den Pol, 2012); release sites per terminal (Ludwig and Leng, 2006; van den Pol, 1982, 2012; Pow and Morris, 1989); co-occurrence of small clear vesicles (van den Pol, 2012); mitochondrial density (Dayanithi et al., 2012; van den Pol, 1982); anatomical location (Castel et al., 1988; Krieg, 1932; van den Pol, 1982; Swanson and Kuypers, 1980); projections to posterior pituitary (Sawchenko and Swanson, 1982; Swanson and Kuypers, 1980); acts peripherally (Kamm et al., 1928; Lambert et al., 1993; Ott and Scott, 1911; Pedersen et al., 1982); cell body diameter (Castel et al., 1988; Krieg, 1932; Xiao et al., 2017); and electrophysiological signature (Eliava et al., 2016; Luther and Tasker, 2000; Xiao et al., 2017). Abbreviations: Nucleus Accumbens (NAc), Paraventricular nucleus (PVN), Supraoptic Nucleus (SON), Ventral Tegmental Area (VTA), Large Dense Core Vesicle (LDCV), Medium Dense Core Vesicle (MDCV). Notes: *validated in current study; †discovered in current study. Adapted from (Dölen, 2015).

**Table S2. HCR probe design.** Related to **Figure 4**, **STAR METHODS**.

| Probe Name | Probe Sequence |
|---|---|
| *Calbindin*_CDS_HCR_B1_P1_odd | GAGGAGGGCAGCAAACGGAATCCTTCCAGGTAACCACTTC |
| *Calbindin*_CDS_HCR_B1_P2_odd | GAGGAGGGCAGCAAACGGAATCTGTCCATATTGATCCACA |
| *Calbindin*_CDS_HCR_B1_P3_odd | GAGGAGGGCAGCAAACGGAAGCTGTGGTCAGTATCATACT |
| *Calbindin*_CDS_HCR_B1_P4_odd | GAGGAGGGCAGCAAACGGAATTCCCACACATTTTGATTCC |
| *Calbindin*_CDS_HCR_B1_P5_odd | GAGGAGGGCAGCAAACGGAAATCTATGTATCCGTTGCCAT |
| *Calbindin*_CDS_HCR_B1_P6_odd | GAGGAGGGCAGCAAACGGAAAGCTTCCCTCCATCCGACAA |
| *Calbindin*_CDS_HCR_B1_P1_even | GGATCAAGTTCTGCAGCTCCTAGAAGAGTCTTCCTTTACG |
| *Calbindin*_CDS_HCR_B1_P2_even | ATTCCTATTTTTCCATCATCTAGAAGAGTCTTCCTTTACG |
| *Calbindin*_CDS_HCR_B1_P3_even | GTTCCTCGGTTTCGATGAAGTAGAAGAGTCTTCCTTTACG |
| *Calbindin*_CDS_HCR_B1_P4_even | CTCAAAAGCCTTATTGAACTTAGAAGAGTCTTCCTTTACG |
| *Calbindin*_CDS_HCR_B1_P5_even | GCAAAGCATCCAGCTCATTTTAGAAGAGTCTTCCTTTACG |
| *Calbindin*_CDS_HCR_B1_P6_even | AAGAGCAAGGTCTGTTCGGTTAGAAGAGTCTTCCTTTACG |
| *Oxt*_CDS_HCR_B3_P1_odd | GTCCCTGCCTCTATATCTTTAGCAAGCGAGACTGGGGCAG |
| *Oxt*_CDS_HCR_B3_P2_odd | GTCCCTGCCTCTATATCTTTTCTGGATGTAGCAGGCCGAG |
| *Oxt*_CDS_HCR_B3_P3_odd | GTCCCTGCCTCTATATCTTTGTCCGAAGCAGCGTCCTTTG |
| *Oxt*_CDS_HCR_B3_P4_odd | GTCCCTGCCTCTATATCTTTGAAGGCAGGTAGTTCTCCTC |
| *Oxt*_CDS_HCR_B3_P5_odd | GTCCCTGCCTCTATATCTTTAGGCGGGGTCTGTGCGGCAG |
| *Oxt*_CDS_HCR_B3_P1_even | AGAGCCAGTAAGCCAAGCAGTTCCACTCAACTTTAACCCG |
| *Oxt*_CDS_HCR_B3_P2_even | CTCTTGCCGCCCAGGGGGCATTCCACTCAACTTTAACCCG |
| *Oxt*_CDS_HCR_B3_P3_even | TCGTCCGCGCAGCAGATGCTTTCCACTCAACTTTAACCCG |
| *Oxt*_CDS_HCR_B3_P4_even | CTTCTGGCCAGACTGGCAGGTTCCACTCAACTTTAACCCG |
| *Oxt*_CDS_HCR_B3_P5_even | GAGAAGGCAGACTCAGGGTCTTCCACTCAACTTTAACCCG |
| *Cnr1*_CDS_HCR_B1_P1_odd | GAGGAGGGCAGCAAACGGAACAAGGCCGTCTAAGATCGACTTCAT |
| *Cnr1*_CDS_HCR_B1_P2_odd | GAGGAGGGCAGCAAACGGAAATCTTCGTACTGAATGTCATTTGAG |
| *Cnr1*_CDS_HCR_B1_P3_odd | GAGGAGGGCAGCAAACGGAACATAAAATTCTCCCCACACTGGATG |
| *Cnr1*_CDS_HCR_B1_P4_odd | GAGGAGGGCAGCAAACGGAAGGAGACTGCGGGAGTGAAGGATGAC |
| *Cnr1*_CDS_HCR_B1_P5_odd | GAGGAGGGCAGCAAACGGAAGTGGAACACGTGGAAGTCAACAAAG |
| *Cnr1*_CDS_HCR_B1_P6_odd | GAGGAGGGCAGCAAACGGAACCACATCAAGCAAAAGGCCACTACG |
| *Cnr1*_CDS_HCR_B1_P7_odd | GAGGAGGGCAGCAAACGGAAACAGATTGCAGCTTCTTGCAGTTCC |
| *Cnr1*_CDS_HCR_B1_P8_odd | GAGGAGGGCAGCAAACGGAACCGATCCAGAACATCAGGTAGGTTT |
| *Cnr1*_CDS_HCR_B1_P9_odd | GAGGAGGGCAGCAAACGGAACAGAGGGCCCCAGCAGATGATCAAC |
| *Cnr1*_CDS_HCR_B1_P10_odd | GAGGAGGGCAGCAAACGGAACGTCTTGATAAGCTTGTTCATCTTC |
| *Cnr1*_CDS_HCR_B1_P11_odd | GAGGAGGGCAGCAAACGGAACATGAAGGGAACATGCTGCGGAAAG |
| *Cnr1*_CDS_HCR_B1_P1_even | TGGTGATGGTACGGAAGGTGGTATCTAGAAGAGTCTTCCTTTACG |
| *Cnr1*_CDS_HCR_B1_P2_even | TAATTTGGATGCCATGTCTCCTTTGTAGAAGAGTCTTCCTTTACG |
| *Cnr1*_CDS_HCR_B1_P3_even | ATTCAGAATCATGAAGCACTCCATGTAGAAGAGTCTTCCTTTACG |
| *Cnr1*_CDS_HCR_B1_P4_even | CAATGAAGTGGTAGGAAGGCCTGCATAGAAGAGTCTTCCTTTACG |
| *Cnr1*_CDS_HCR_B1_P5_even | CAGAAACACATTGGGACTATCTTTGTAGAAGAGTCTTCCTTTACG |
| *Cnr1*_CDS_HCR_B1_P6_even | CAACACAGCAATTACTATTGCAATATAGAAGAGTCTTCCTTTACG |
| *Cnr1*_CDS_HCR_B1_P7_even | TCAATGAGTGGGAAGATGTCTGAGCTAGAAGAGTCTTCCTTTACG |
| *Cnr1*_CDS_HCR_B1_P8_even | ATGAACAGCAACAGCACACTGGTGATAGAAGAGTCTTCCTTTACG |
| *Cnr1*_CDS_HCR_B1_P9_even | AAAGACATCATACACCATGATCGCATAGAAGAGTCTTCCTTTACG |
| *Cnr1*_CDS_HCR_B1_P10_even | GCAGAGCATACTACAGAAGGCAAACTAGAAGAGTCTTCCTTTACG |
| *Cnr1*_CDS_HCR_B1_P11_even | TTATCTAGAGGCTGCGCAGTGCCTTTAGAAGAGTCTTCCTTTACG |